

011 This work, intends to improve a monocular region-based tracking algo-
 012 rithm using an RGB camera. The algorithm to be improved, derives from
 013 a particle filter where each particle represents a hypothesis of the state of
 014 the object in 3D. However, the literature mentions that the particle filter
 015 (PF) uses a very limited importance distribution to propagate the parti-
 016 cles, which easily leads the filter to degenerate and loose track of the
 017 object. Given the limitation of the PF, an unscented particle filter (UPF)
 018 is proposed. This one obtains an approximation to the optimal importance
 019 distribution, by adding a current observation of the state.

020 In order to compare the proposed algorithm with the previous one,
 021 both are implemented and several real and simulated experiments with a
 022 simple object are performed. From the results obtained, is shown that the
 023 filters are successful, with the UPF being more robust.

024 1 Introduction

025

026 The most known methods to track an object using an RGB camera, are
 027 the methods based on 3D reconstruction and the ones based on test hy-
 028 pothesis. The first methods, start by using the visual information of the
 029 2D image to reconstruct the pose of the object in 3D and the other ones,
 030 consists in generating numerous hypothesis about what could be the ex-
 031 act state of the object in 3D, and test each hypothesis from the 2D image
 032 information. The advantages of 3D reconstruction is that it's fast and
 033 easy to localize the object of interest, however, they are easily affected by
 034 noise in the image. On the other hand, the last methods are more precise
 035 because the image's noise is not taken into account, yet, they are very
 036 slow and poor in localizing the object. The main intent to use the UPF is
 037 to combine both methods to get the advantages of both. Thus, by defin-
 038 ing the particles as 3D object's state hypothesis and introducing a current
 039 measurement of the object's state through a 3D reconstruction process, an
 040 hybrid algorithm is formulated.

041 In Bayes perspective and under the Markov assumption, the problem
 042 is to recursively estimate the posterior distribution of the current state
 043 \mathbf{x}_t conditioned on all available observations $\mathbf{z}_{1:t} = \{\mathbf{z}_1, \dots, \mathbf{z}_t\}$. One just
 044 needs to define some initial prior $p(\mathbf{x}_0)$, state transition $p(\mathbf{x}_t|\mathbf{x}_{t-1})$, and
 045 observation $p(\mathbf{z}_t|\mathbf{x}_t)$ probabilities, in mathematical terms [5]:

$$046 p(\mathbf{x}_t|\mathbf{z}_{1:t}) \propto p(\mathbf{z}_t|\mathbf{x}_t) \int p(\mathbf{x}_t|\mathbf{x}_{t-1})p(\mathbf{x}_{t-1}|\mathbf{z}_{1:t-1})d\mathbf{x}_{t-1}. \quad (1)$$

047 However, the equation (1) is intractable, and for this reason many kind of
 048 numerical approximations, like the methods based on particles, have been
 049 developed. They represent the posterior distribution as N weighted set of
 050 Monte Carlo samples $\{\mathbf{x}_t^{(i)}, w_t^{(i)}\}$, $i = 1, \dots, N$, also known as particles,
 051 and by the law of the big numbers, the bigger the number of particles the
 052 lower is the variance of the approximation error [6]. Unfortunately, it's
 053 often impossible to sample directly from the posterior distribution, so a
 054 known and easy-to-sample distribution $q(\mathbf{x}_t^{(i)}|\mathbf{x}_{0:t-1}, \mathbf{z}_{1:t})$, called impor-
 055 tance distribution is applied. By drawing samples from this distribution,
 056 a recursive estimate for the importance weights can be derived [6]:

$$057 w_t^{(i)} \propto \frac{p(\mathbf{z}_t|\mathbf{x}_t^{(i)})p(\mathbf{x}_t^{(i)}|\mathbf{x}_{t-1}^{(i)})}{q(\mathbf{x}_t^{(i)}|\mathbf{x}_{0:t-1}, \mathbf{z}_{1:t})} w_{t-1}^{(i)}. \quad (2)$$

058 This type of methods exhibit a phenomenon called degeneration. This
 059 happens when some particles get all the weight and a lot of them get
 060 insignificant. To prevent this, a process of resampling is implemented
 061 to replicate the particles with high weights and discard the lower ones
 062

[6]. Doing this, brings more particles to regions of high likelihood, which
 not only contributes to get better estimates, but also to avoid the particles
 from moving wrongly in the state space. One filter that derives from these
 type of methods, is the particle filter, that uses the simple state transition
 probability as the importance distribution. Yet, the literature mentions
 that in this type of methods, the most critical design issue is the choice of
 importance distribution. If the likelihood function is too narrow, or if it lies
 in one of the tails of the prior distribution, even the resampling process
 might not be enough to prevent degeneration [6]. In a Markov process,
 the optimal importance distribution in terms of minimizing the variance of
 the weights is given by:

$$q(\mathbf{x}_t|\mathbf{x}_{0:t-1}, \mathbf{z}_{1:t}) = p(\mathbf{x}_t|\mathbf{x}_{t-1}, \mathbf{z}_t). \quad (3)$$

However, sampling from this distribution is non-trivial, because of the
 dependence on the actual observation \mathbf{z}_t , thus, with the intent of getting an
 approximation to this distribution, the unscented particle filter introduced
 by Van Der Merwe *et al.* [6] was developed. This one uses the unscented
 kalman filter (UKF), which introduces a current observation together with
 a Gaussian approximation of the state, as the importance distribution to
 propagate each particle [6]:

$$q(\mathbf{x}_t^{(i)}|\mathbf{x}_{0:t-1}^{(i)}, \mathbf{z}_{1:t}) = \mathcal{N}(\mu_t^{(i)}, \mathbf{P}_t^{(i)}), i = 1, \dots, N. \quad (4)$$

024 2 Methodology

The algorithm to be improved in this work is the one developed by M. Ta-
 iana *et al.* [5], in which to track a homogeneous ball, the state is defined as
 the position and velocity of the ball in space $\mathbf{x}_t = [x \ y \ z \ \dot{x} \ \dot{y} \ \dot{z}]^T$.
 The algorithm is based on a particle filter, where each particle represents
 a 3D hypothesis of the ball's state, this allows one to overcome the in-
 version of the nonlinearity caused by the camera projection model and
 enables the use of realistic 3D motion models as the state transition prob-
 ability [5]. On the observation model, each particle project a few tens of
 points onto the current image of a video frame from his state hypothesis,
 one set inside and the other outside the 3D object's silhouette. With the
 chromatic information of these points, a normalized color histogram for
 the inner region and another for the outer region, are constructed along
 with the normalized color histogram of the object's color model [5]. The
 likelihood of a particle is considered high, if the inner and model histo-
 grams are similar and at the same time, the inner and outer histograms
 are different. To express this mathematically, a metric \mathcal{D} is constructed,
 based on the Bhattacharyya coefficient that quantifies the similarity be-
 tween histograms. At last, the observation probability of each particle is
 modeled by a Laplacian distribution over the metric \mathcal{D} , where ε was set
 to $\varepsilon = 1/30$ [5]:

$$p(\mathbf{z}_t|\mathbf{x}_t^{(i)}) \propto e^{-\frac{\mathcal{D}}{\varepsilon}}. \quad (5)$$

024 2.1 Proposed algorithm

On the previous algorithm, a motion model is applied to predict the next
 state of the particles, for the UPF, it's the unscented kalman filter that
 is used. This filter returns a prediction considering a motion model and a
 current observation, where the observation is a measure of the 3D position
 of the ball. The measurement process, consists in a method to estimate
 the current 3D position of the ball from an image. In order to accomplish
 this, a few steps must take place. The method first starts with color seg-
 mentation to identify the whereabouts of the ball. The ball is identified
 in the image through the highest pixel probability, corresponding to the

reference histograms created based on the ball's color model, and the image is then binarized with the use of Otsu threshold [3] to distinguish the ball from the background. Next, with the use of morphological operators, the possible noise that survived the threshold, is removed and the edges of the ball smoothed. The contour is extracted with the Moore Neighborhood [4] tracing algorithm and these points are used to extract an ellipse with the RANSAC [2] algorithm. With the best fitted ellipse, the 3D position is then obtained through monocular reconstruction [1] that uses the prior information of the ball radius and camera parameters to estimate a position from the ellipse fitted to the blob.

3 Results & Discussion

In order to access and compare the performance of the PF and UPF, several tests over simulated trajectories and real experiments were made. Results for a simulated circular trajectory and for a real free-fall trajectory are shown in this section. For both filters, there are adjustments parameters that affects the performance. The principal and only parameters tested are: the number of particles (the higher the number the better are the estimates), the distance between the inner and outer points (that controls the measurement error) and the process model noise (that regulates the dispersion of the particles in the state space). For all the plots, the tests were made using $N = 1024$ particles, where the red lines represent closer inner and outer points, the green corresponds to points a bit more distant than the red ones, and the blue even more distant. The solid, dashed and dotted lines, represent three different process noise configurations. For all tests, the motion model used corresponds to a constant velocity model. To analyze the influence of the number of particles, the root mean square error (RMSE) was used and to examine the influence of the silhouette distances and process noises, precision plots were created. This plots instead of the RMSE, can catch if a filter loses track of an object, and for filters like these, this scenario often happens. Precision plots express the percentage of estimates that possess an error below a given error threshold, as the error threshold increases. The considered error threshold is the relative error δ . Therefore, the following equation is used to compute the percentage of the estimates F , that possess an error below an arbitrary relative error δ :

$$F = \frac{100}{N} \sum_{i=1}^N H \left(\delta - \frac{\|\mathbf{x}_i - \hat{\mathbf{x}}_i\|}{\|\mathbf{x}_i\|} \right) \quad [\%] \quad (6)$$

where H is the Heaviside function, N represents the number of estimates that belong to the experience, and \mathbf{x}_i and $\hat{\mathbf{x}}_i$ corresponds respectively, to the exact state and the state estimate i . Both filters deal with random variables, thus, making tests with the same parameters originates different results and for this motive each test is repeated 100 times.

N	128	256	1024
PF	6.32×10^8	392.35	24.13
UPF	27.05	26.04	23.98

Table 1: RMSE error in mm using different number of particles.

In the table 1 are exposed results of RMSE of the position estimations for a given experience, varying only the number of particles. One can verify that the results coincides with the literature, once as the number of particle increases, better are the estimates, but the lower is the computational efficiency. Comparing the real results against the simulated ones (figure 1 and figure 2), it is quite visible, that for the real experiences, the relative error is bigger, at least the double, which make sense, because the simulator does not take into account the real phenomena of the world. Other aspect is the high sensitivity that the PF exhibits for different process noises and different distances between the inner and outer points (see figure 1(a)). For this filter, the process noise is directly related to the acceleration of the object and for one order of magnitude below or above the process noise used by the solid lines, the filter loses track of the ball and degenerates, which leads to wrong estimates. For the dotted lines the problem is the low scattering of the particles, and so, the filter cannot keep up with the object's movement. For the dashed lines the particles get scattered too much and deviate from the ball which degenerates the filter. For the UPF the estimates of the position are all adequate for different process models. The real trajectory is a free-fall in which the ball collides with the ground multiple times, that makes the ball to rapidly change it's

movement. That's why for the PF, the obtained results are very poor (see figure 2(a)). After an impact, the particles easily loose track of the ball and hardly recover to regions of high likelihood. On the other hand, one can see the real advantage of the UPF. If the particles loose track of the ball (mainly after an impact), the current observation acquired from a 3D reconstruction based method that easily localize the ball, will pull the particles to regions of high likelihood. Despite using such a limited motion model for this trajectory, the UPF obtains satisfactory results (see 2(b)).

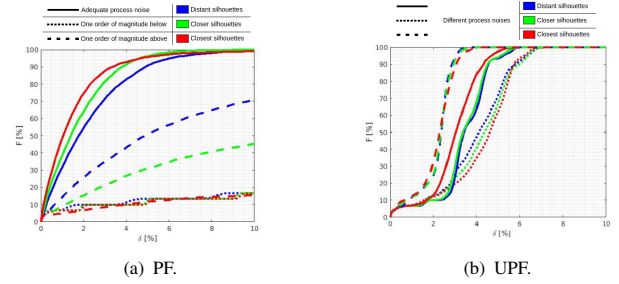


Figure 1: Position estimates for the simulated circular trajectory.

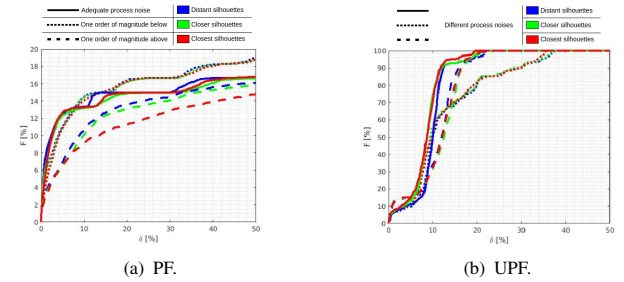


Figure 2: Position estimates for the real free-fall trajectory.

4 Conclusions

The results obtained in this work, allows one to conclude that the implemented filters function with success, if the filters initial parameters are adjusted accordingly to the object's trajectory. For high uncertainty trajectories like a free-fall, the PF easily degenerates, contrarily, the UPF was successfully in all tests for any trajectory, which allows one to conclude that it's way more robust against all the three tested parameters. As future work, different observation models can be developed in order to make the algorithms usable for more complex objects.

Acknowledgements

This work was supported by:
FCT with the LARSyS - FCT Project UIDB/50009/2020.

References

- [1] N. Greggio and J. Gaspar *et al.* Monocular vs binocular 3d real-time ball tracking from 2d ellipses. In *ICINCO 2011 - Proceedings of the 8th International Conference on Informatics in Control, Automation and Robotics*, volume 2, June 2011.
- [2] K. Kanatani, Y. Sugaya, and Y. Kanazawa. Ellipse Fitting. In *Guide to 3D Vision Computation. Advances in Computer Vision and Pattern Recognition*, pages 11–32. Springer, Cham, 2016.
- [3] N. Otsu. A threshold selection method from gray-level histograms. *IEEE Transactions on Systems, Man, and Cybernetics*, 9(1):62–66, 1979.
- [4] P. Reddy and V. Amarnadh *et al.* Evaluation of Stopping Criterion in Contour Tracing Algorithms. *International Journal of Computer Science and Information Technologies*, 3(3):3888–3894, 2012.
- [5] Matteo Taiana and Joao Santos *et al.* Tracking objects with generic calibrated sensors: An algorithm based on color and 3d shape features. *Robotics and Autonomous Systems*, 58(6):784 – 795, 2010.
- [6] R. Van Der Merwe and A. Doucet *et al.* The unscented particle filter. In *Proceedings of the 13th International Conference on Neural Information Processing Systems*, page 563–569, Cambridge, MA, USA, 2000. MIT Press.

063
064
065
066
067
068
069
070
071
072
073
074
075
076
077
078
079
080
081
082
083
084
085
086
087
088
089
090
091
092
093
094
095
096
097
098
099
100
101
102
103
104
105
106
107
108
109
110
111
112
113
114
115
116
117
118
119
120
121
122
123
124
125
*/